Heliyon 10 (2024) e30827

Contents lists available at ScienceDirect

Heliyon

journal homepage: www.cell.com/heliyon

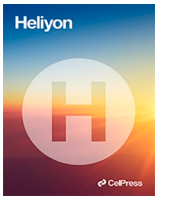

Research article

Characterization of a predictive signature for tumor microenvironment and immunotherapy response in hepatocellular carcinoma involving neutrophil extracellular traps

Ziwei Yuan [a,b,1], Xuejia Yang [a,1], Zujian Hu [a], Yuanyuan Gao [a], Penghua Yan [a], Fan Zheng [a], Yangyang Guo [c,*], Xiaowu Wang [d,**], Jingzong Zhou [b,***]

[a] *Key Laboratory of Diagnosis and Treatment of Severe Hepato-Pancreatic Diseases of Zhejiang Province, The First Affiliated Hospital of Wenzhou Medical University, Wenzhou, 325000, China*
[b] *Department of Endocrinology, Taizhou Hospital of Zhejiang Province Affiliated to Wenzhou Medical University, Taizhou, Zhejiang, China*
[c] *Department of General Surgery, Ningbo First Hospital, Ningbo, 315000, China*
[d] *Department of Burns and Skin Repair Surgery, The Third Affiliated Hospital of Whenzhou Medical University, Ruian, 325200, Zhejiang Province, China*

ARTICLE INFO

Keywords:
NETs
Hepatocellular carcinoma
Immune microenvironment
Immunotherapy
Prognosis

ABSTRACT

Neutrophil extracellular traps (NETs) and other factors play a significant role in impacting the prognosis of patients with Hepatocellular carcinoma (HCC). Nevertheless, further research is warranted to fully elucidate the prognostic implications of NETs in patients with HCC. We employed a hierarchical clustering technique to examine the Cancer Genome Atlas-Liver Hepatocellular Carcinoma (TCGA-LIHC) data and identified subtypes associated with NETs. Subsequently, we utilized LASSO regression analysis to identify a distinct gene expression pattern within these subtypes. The strength of this signature was further validated through analysis of TCGA-LIHC and International Cancer Genome Consortium-Liver Cancer (ICGC-LIRI-JP) data. Our findings resulted in the construction of a six-gene signature related to NETs, which can predict survival outcomes in HCC patients. To enhance the predictive accuracy of our tool, we developed a nomogram that integrates the NETs signature with clinicopathological characteristics. We validated the significance of NETs in HCC patients using qRT-PCR and immunohistochemistry assays, along with in vitro experiments targeting high-risk genes. Furthermore, our exploration of the immune microenvironment uncovered augmented immune-specific metrics within the low-risk cohort, implying potential disparities in immune-related attributes between the high-risk and low-risk contingents. In summary, the NETs signature we discovered serves as a valuable biomarker and provides guidance for personalized therapy in HCC patients.

* Corresponding author.
** Corresponding author.
*** Corresponding author.
E-mail addresses: yang984054863@163.com (Y. Guo), wangxiaowu_email@163.com (X. Wang), 785506003@qq.com (J. Zhou).
[1] These authors contributed equally to this work and should be considered joint first authors.

https://doi.org/10.1016/j.heliyon.2024.e30827
Received 18 September 2023; Received in revised form 26 April 2024; Accepted 6 May 2024
Available online 8 May 2024

1. Introduction

Primary hepatic malignancy, colloquially known as hepatocellular carcinoma (HCC), constitutes approximately 75 %–80 % of cases and was responsible for around 841,000 new cases globally in 2018, ranking it as the sixth most prevalent malignancy. Moreover, HCC is responsible for approximately 782,000 fatalities annually, rendering it the fourth most lethal cancer. The incidence of HCC is on a relentless upward trajectory, accompanied by a concerning rise in associated mortality rates [1]. The main treatment for HCC is surgery, with additional interventions such as interventional therapy, radiotherapy, chemotherapy, targeted drugs, and immunotherapy. However, the prognosis for HCC remains poor due to frequent recurrence and metastasis, resulting in a less than 18 % five-year survival rate [2]. Traditionally, prognostic assessment of patients with HCC has been heavily reliant upon the Tumor-Node-Metastasis (TNM) staging system, which has limitations as it only examines the prognosis of patients at a broader scale [3]. With the advancement of gene detection and molecular targeted therapy, the gene expression-based evaluation of prognosis is currently a research hotspot [4].

Neutrophil extracellular traps (NETs) form when activated neutrophils release granular proteins and chromatin [5]. The formation of NETs entails neutrophil demise, a process termed NETosis, which is distinct from apoptosis and necrosis [6,7]. It is important to note that NETs occur in many other diseases, including cancer, rheumatoid arthritis, and thrombosis [8–10]. Mounting evidence suggests that NETs are implicated in the progression and dissemination of cancer [11,12]. Additionally, NETs promote the inflammatory response of HCC tumors and their metastatic potential [13]. However, the extent to which NETs exert a definitive influence on the pathogenesis and prognostic trajectory of HCC continues to elude our full understanding.

The objective of this study was to predict the outcomes and effectiveness of immunotherapy in HCC patients by using molecular clustering and prognostic features of NETs. Firstly, HCC patients were categorized into two distinct non-redundant NETs clusters based on their expression profiles. Subsequently, we identified marker genes strongly correlated with NETs, which served as predictive markers for patient survival in HCC. To enhance the clinical applicability of our findings, we developed a chart combining NETs markers with clinical pathological features, thereby improving the predictive accuracy. To further validate the significance of NETs in HCC, we conducted qRT-PCR and immunohistochemistry experiments, as well as in vitro experiments targeting high-risk genes. These experiments offer further substantiation for the involvement of NETs in HCC progression, underscoring their potential as viable therapeutic targets. Furthermore, we investigated the immune microenvironment surrounding HCC tumors and discovered significant differences in immune scoring between high-risk and low-risk groups, suggesting potential variations in immune-related characteristics. This finding emphasizes the complex interplay among NETs, tumor microenvironment, and immune response in HCC. In summation, our study offers significant insights into personalized treatment strategies for HCC by elucidating the importance of NETs and identifying marker genes associated with NETs, thus contributing to improved prognosis and treatment efficacy.

2. Approaches and procedures

2.1. Data extraction and process

Gene expression data in the Fragments Per Kilobase of transcript per Million mapped reads (FPKM) format were acquired from The Cancer Genome Atlas database (TCGA-LIHC, https://portal.gdc.cancer.gov). 370 HCC tumor samples and 53 normal samples, along with their respective clinical information are included in this dataset. A colon was used to introduce the source of the data: R software was used to split TCGA-LIHC into training and test groups, with a ratio of 1:1 (see Supplementary Table S1). Additionally, 232 HCC tumor samples along with their corresponding prognostic data were retrieved from the ICGC database (ICGC-LIRI-JP) for external validation. Within Supplementary Tables S2 and 69 associated genes, as identified in an earlier study, are additionally cataloged [14].

2.2. Consensus clustering of NETs-associated genes

Cluster classification of HCC was performed using the R packages "limma" and "ConsensusClusterPlus" [15]. We used the R package 'survival' to examine the correlation between clusters and overall survival rate. Single quotation marks were used around "survival". Heat maps and Kaplan-Meier curves were created using the R packages 'pheatmap', 'survival', and 'survminer' [16]. Differential gene expression was assessed using the 'limma' package, identifying genes with an absolute log fold change (FC) > 1 and an FDR <0.05 as differentially expressed genes (DEGs) between the two clusters. Leveraging the CIBERSORT algorithm as a molecular scalpel, we meticulously dissected the differential distribution of immune cell subsets between the designated cohorts, thereby elucidating the intricate variations in immune cell infiltration patterns.

2.3. Identification of the NETs-related signature

Prognostic DEGs were identified via univariate Cox regression analysis. To construct a NETs-related signature, a rigorous two-step process was meticulously implemented. Firstly, LASSO regression analysis was employed, followed by multivariate Cox regression, culminating in the selection of six genes that collectively define this unique molecular signature [17,18]. Employing their median expression levels as the demarcation point, HCC patients were meticulously classified into two distinct subgroups. Subsequently, Kaplan-Meier analysis was conducted to perform an in-depth comparison of overall survival rates between these subgroups. Leveraging the statistical prowess of the 'survival', 'survminer', and 'timeROC' R packages [19], comprehensive subgroup analyses were conducted to assess overall survival. Furthermore, receiver operating characteristic (ROC) curves were generated to assess the

predictive performance of the NETs-related risk score. To facilitate clinical decision-making, a comprehensive nomogram was developed, incorporating the NETs-related risk score alongside other clinically relevant factors. The accuracy of this nomogram was rigorously assessed through the construction of a calibration graph and multifactor ROC analyses at various follow-up intervals, including 1-, 3-, and 5-year timepoints.

2.4. Immune microenvironment characterization

To elucidate the immunological landscape of distinct subgroups, a multipronged approach was employed. The ESTIMATE algorithm quantified the relative abundance of immune cells (ImmuneScores) and stromal cells (StromalScores) within the tumor microenvironment [20]. To evaluate the distinct immune cell infiltration pattern between different subgroups, we performed MCPCOUNTER, QUANTISEQ, EPIC, XCELL, TIMER, CIBERSORT, and CIBERSORT-ABS analyses. We employed single-sample gene set enrichment analysis (ssGSEA) to discern variations in immune cell infiltration and immune function across the two groups [21]. Moreover, the Immunophenoscore (IPS) gauged the susceptibility to immunotherapy in high-risk and low-risk subgroups [22,23].

2.5. Enrichment profiling of the NETs signature

DEGs between high- and low-risk HCC were identified by screening the TCGA-LIHC dataset. In subsequent analyses, gene ontology (GO) and the Kyoto Encyclopedia of Genes and Genomes (KEGG) were harnessed to elucidate enriched pathway signatures associated with the differentially expressed genes. To delineate the functional divergence between high-risk and low-risk patients, gene set variation analysis (GSVA) was meticulously employed to unravel disparities in potential biological function.

2.6. Pharmacodynamic sensitivity profiling

We investigated the predictive ability of a NETs signature for both chemotherapy and targeted therapeutics. An algorithm utilizing the 'pRRophetics' R package was employed to compare drug sensitivity between subtypes. Half-maximal inhibitory concentration (IC50) values serve as a quantitative metric of drug efficacy in modulating specific biochemical or biological processes, providing a measure of the drug's potency in inhibiting a given molecular target [24].

2.7. Quantitative real-time PCR analysis (qRT-PCR)

A total of eight tumor samples and eight control samples were collected from patients diagnosed with liver cancer at the First Hospital of Ningbo City (License number: 068A01). Total RNA was extracted from the experimental samples using Trizol reagent (Glpbio, California, USA), adhering to the manufacturer's prescribed protocol. Reverse transcription was performed using Vazyme's procedure to synthesize cDNA. Target gene quantification was achieved utilizing the SYBR Green Mix Kit (Vazyme), with β-actin serving as the reference gene for normalization. Relative gene expression levels were calculated using the $2^{-\Delta\Delta Ct}$ method.

2.8. Immunohistochemistry staining

Following the instructions provided by the reagent manufacturer, liver tissue sections from patients with hepatocellular carcinoma were dewaxed and rehydrated, followed by antigen retrieval using citric acid. Subsequently, the sections were blocked with hydrogen peroxide and goat serum. After overnight incubation at 4 °C with primary antibodies (CYP26B1, CCR7, CABYR, SLC1A5, HAVCR1, and STC2) (1:100 dilution), the sections were washed. Horseradish peroxidase-conjugated secondary antibodies were subsequently incubated with the sections at 37 °C for a duration of 1 h. Immunohistochemical staining was performed using hematoxylin and diaminobenzidine (DAB) as the chromogen. Image acquisition was performed using a Leica microscope.

2.9. Cell culture and treatment

Huh7 human hepatoma cells, sourced from the FuHeng Cell Center in Shanghai, China, were maintained in Dulbecco's Modified Eagle Medium (DMEM) supplemented with 10 % fetal bovine serum (FBS) from Gibco, USA. Cells were cultured under standard conditions at 37 °C in a humidified atmosphere with 5 % CO2. Transfection experiments were performed by introducing siRNA targeting the HAVCR1 gene into Huh7 cells using Lipofectamine 2000 reagent (Invitrogen, USA). Post-transfection, cell supernatants were collected and analyzed for NETs using an enzyme-linked immunosorbent assay (ELISA) kit (Beyotime, China). The assessed markers included MPO-DNA complexes and neutrophil elastase (NE). The assay was performed following the kit's instructions, and the optical density (OD) at 450 nm was measured in the final step. Cell viability assessments were performed in accordance with the manufacturer's protocol utilizing the Cell Counting Kit-8 (CCK-8) (Beyotime, China). Absorbance measurements were subsequently obtained at a wavelength of 450 nm.

2.10. Statistical analysis

GraphPad Prism 9 and R software (version 3.6.2) were performed for conducting the statistical analyses. The software tools were used to compare the two groups under investigation. Significant differences were determined using either the Wilcoxon test or *t*-test

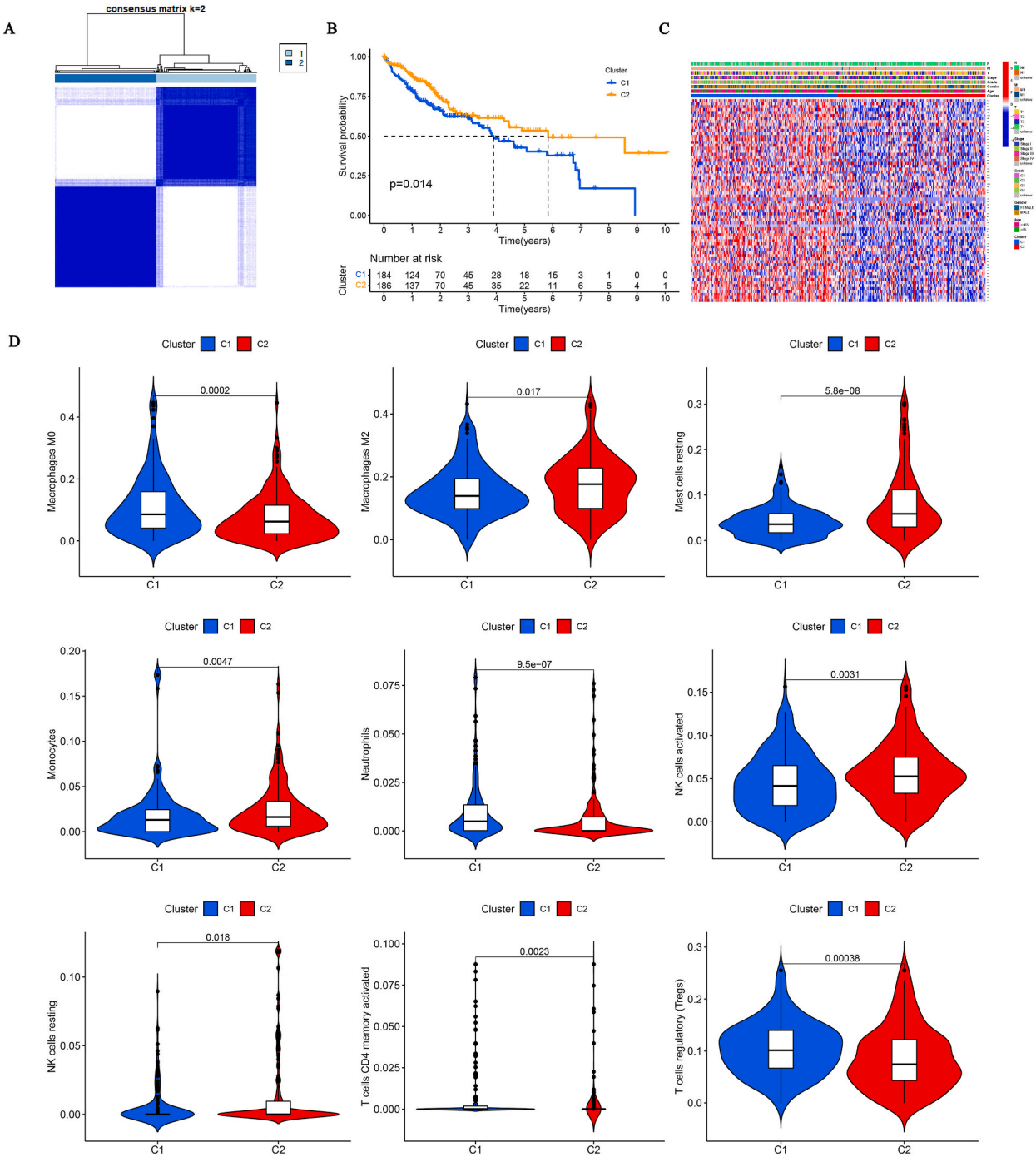

Fig. 1. NETs clusters and clinical characteristics between HCC samples in two clusters. (A) Two NETs clusters were defined using consensus clustering analyses. (B) KM curve indicated that NETs cluster 2 had a longer survival time than NETs cluster 1. (C) Heatmaps showed the relationship between NETs clusters and clinical features and NETs expression in HCC patients. (D) The differences in immune cell infiltration between the two clusters.

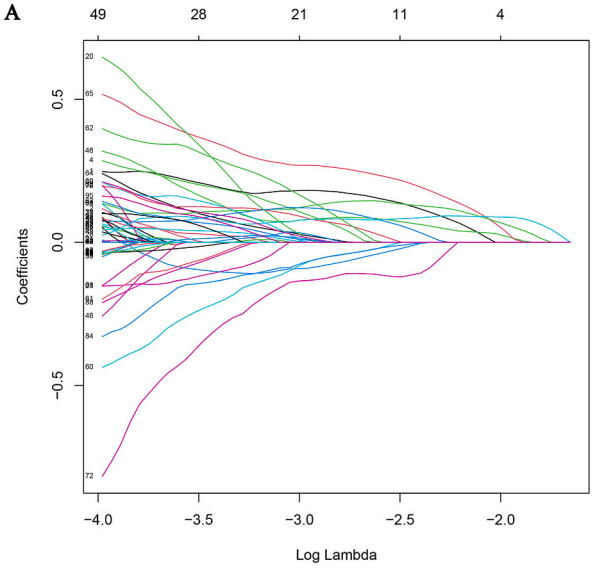

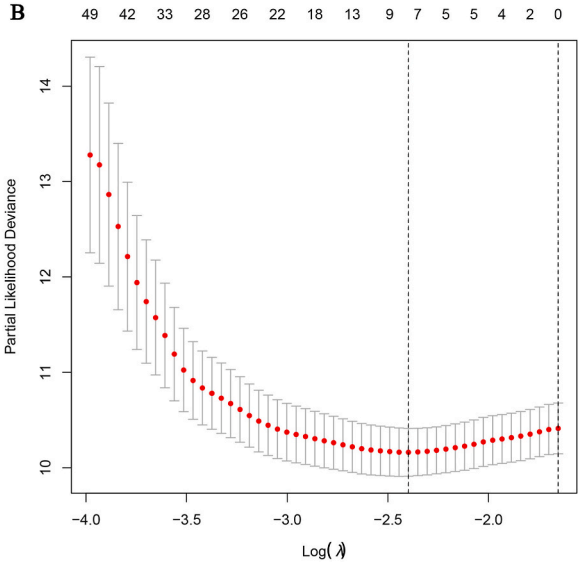

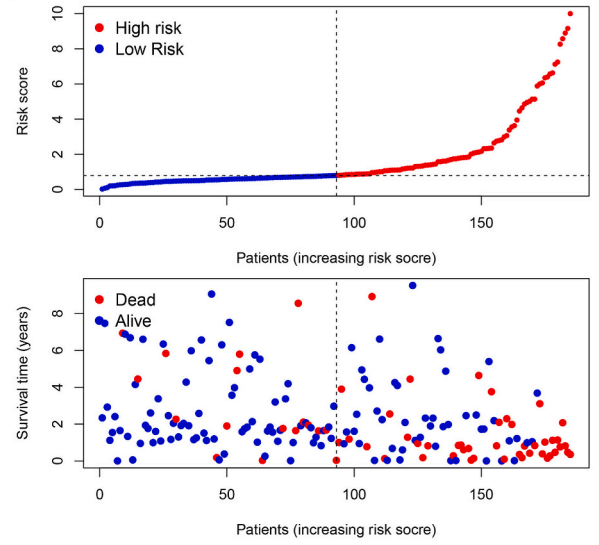

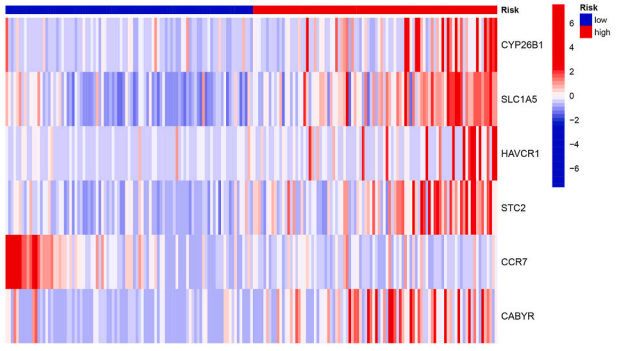

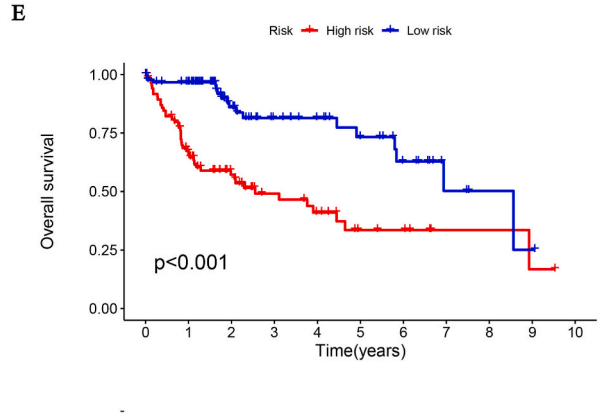

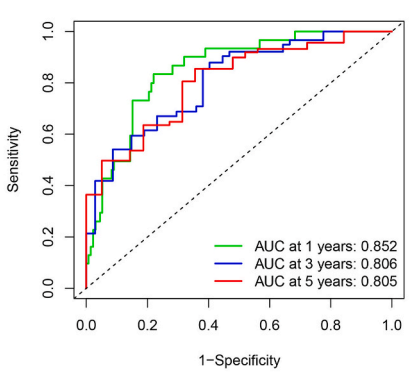

(caption on next page)

Fig. 2. Construction of the prognostic signature. (A) LASSO coefficient profiles (y-axis) of the gene sets and the optimal penalization coefficient (l) via 3-fold cross-validation based on partial likelihood deviance. (B) The dotted vertical lines represent the optimal values of l. The top x-axis has the numbers of gene sets, while the lower x-axis displays the logarithm of λ. (C) The risk score and its corresponding survival outcomes for each case are presented. (D) The heatmap displays the expression levels of six genes among two risk groups. (E) The K-M curve demonstrates a worse prognosis for patients in the high-risk group. (F) The AUC values for 1-year, 3-year, and 5-year survival.

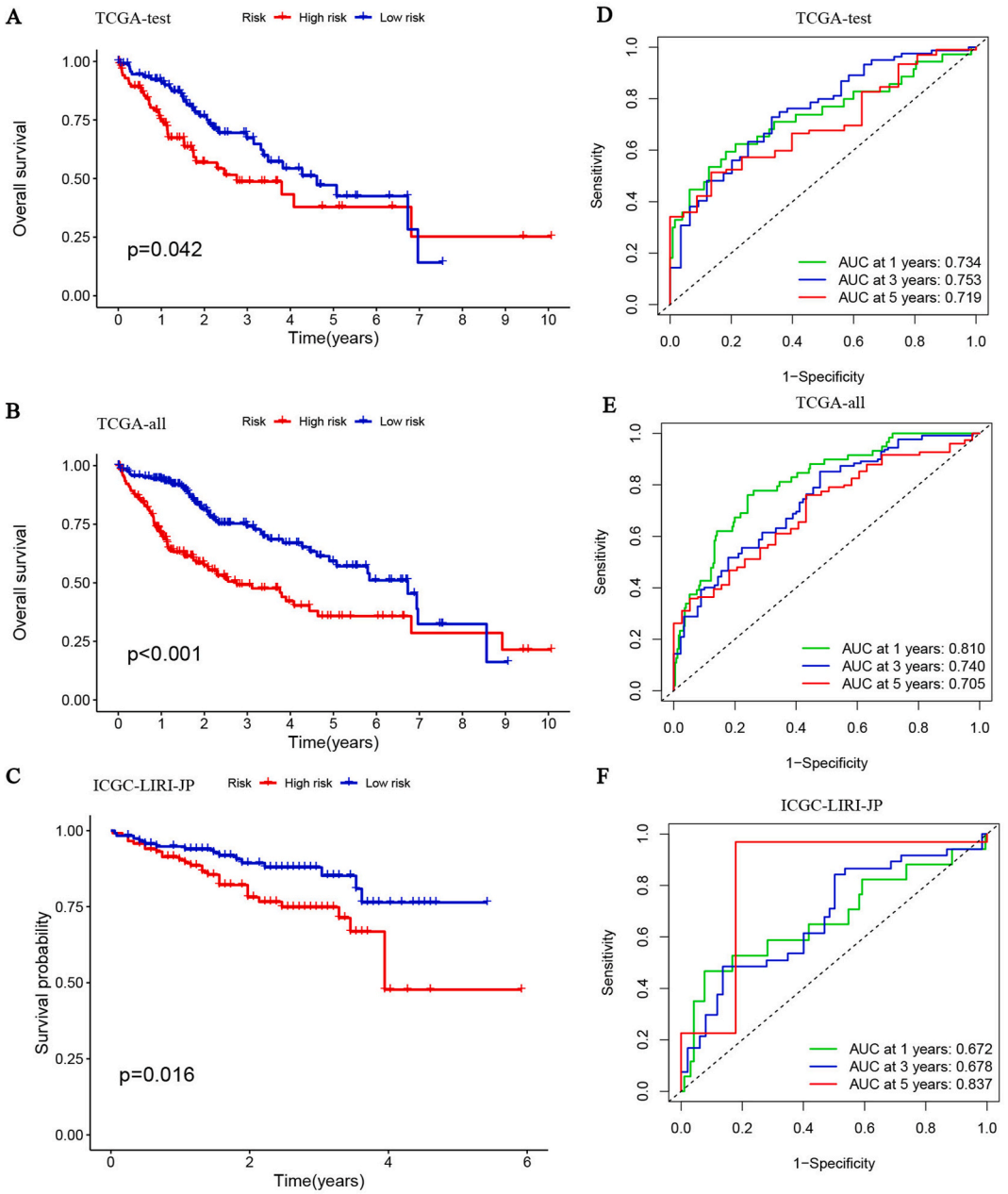

Fig. 3. Validation of the prognostic signature. (A, B, C) Kaplan-Meier (KM) curves indicate that patients in the high-risk group had a worse prognosis in TCGA-test, TCGA-all, and ICGC-LIRI-JP datasets. (D, E, F) The AUC values for 1-year, 3-year, and 5-year survival in TCGA-test, TCGA-all, and ICGC-LIRI-JP datasets are provided.

depending on data distribution. *P* values less than 0.05 were deemed statistically significant, ensuring reliable results.

3. Results

3.1. NETs-related consensus clusters in HCC

To examine how NETs-related gene expression correlates with the classification of HCC, we conducted consensus clustering analysis. TCGA-LIHC was divided into two subgroups (C1 and C2) based on the expression of genes related to NETs, as shown in Fig. 1A. We observed a significantly worse overall survival (OS) of HCC in subgroup C1 compared to C2 (Fig. 1B). Fig. 1C illustrates the interrelationship among NETs clusters, diverse clinical characteristics, and the gene expression associated with NETs.

Given the crucial involvement of immune cells in the development and advancement of HCC, we scrutinized the unique patterns of immune cell infiltration across the two clusters. Cluster 2 exhibited higher proportions of M2 macrophages, NK cells, resting mast cells, and monocytes compared to cluster 1. In contrast, cluster 2 had lower proportions of M0 macrophages, memory CD4 T cells, neutrophils, and Tregs compared to cluster 1. The analysis revealed distinct immune cell populations between the two clusters (Fig. 1D).

3.2. Development of the NETs-related prognostic signature

Subsequently, we performed a univariate Cox analysis and identified 196 prognostic DEGs. This analysis resulted in the

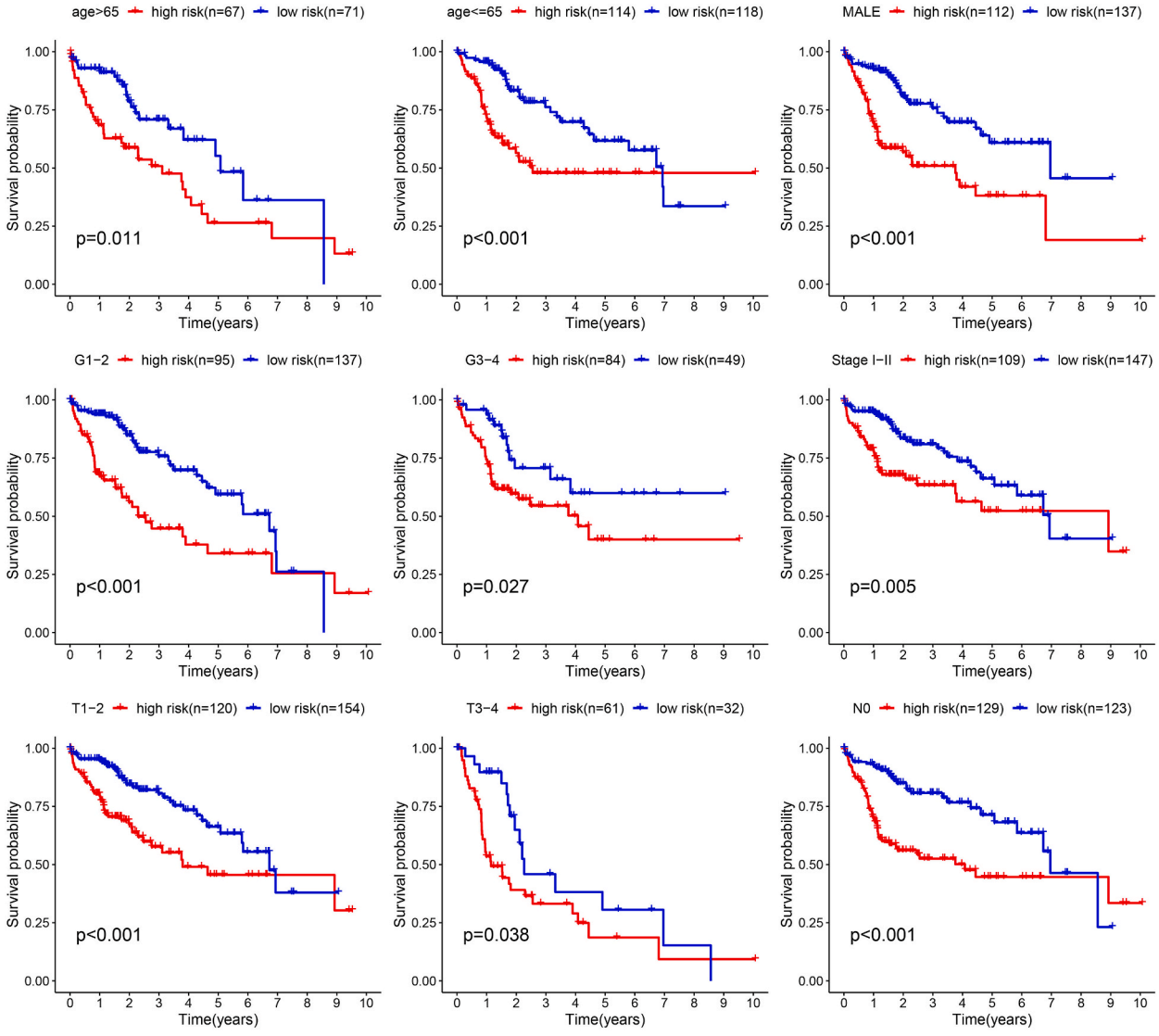

Fig. 4. Validation of the prognostic value of NETs signature in different clinical characteristics groups.

construction of a 6-gene NETs signature (CYP26B1, CCR7, CABYR, SLC1A5, HAVCR1, and STC2) (Fig. 2A and B). Risk score= (CYP26B1 × (0.30454) + SLC1A5 × (0.16716) + HAVCR1 × (0.38717) + STC2 × (0.27510) + CCR7 × (−0.87163) + CABYR × (0.27934)).

Patients with elevated risk scores exhibited a heightened mortality rate compared to their counterparts with diminished risk scores, as determined by the median score (Fig. 2C). We conducted a comparative analysis of the expression levels of these 6 genes between the two distinct risk groups (Fig. 2D). Furthermore, we observed that low-risk patients had a significantly better survival outcome than high-risk patients ($P < 0.001$), as shown in Fig. 2E. The ROC curve demonstrated the stability of the NETs signature, with AUC values of 0.852, 0.806, and 0.805 at 1, 3, and 5 years, respectively, as shown in Fig. 2F.

We subsequently segregated the HCC samples within the test dataset into distinct risk strata: high-risk and low-risk. Our

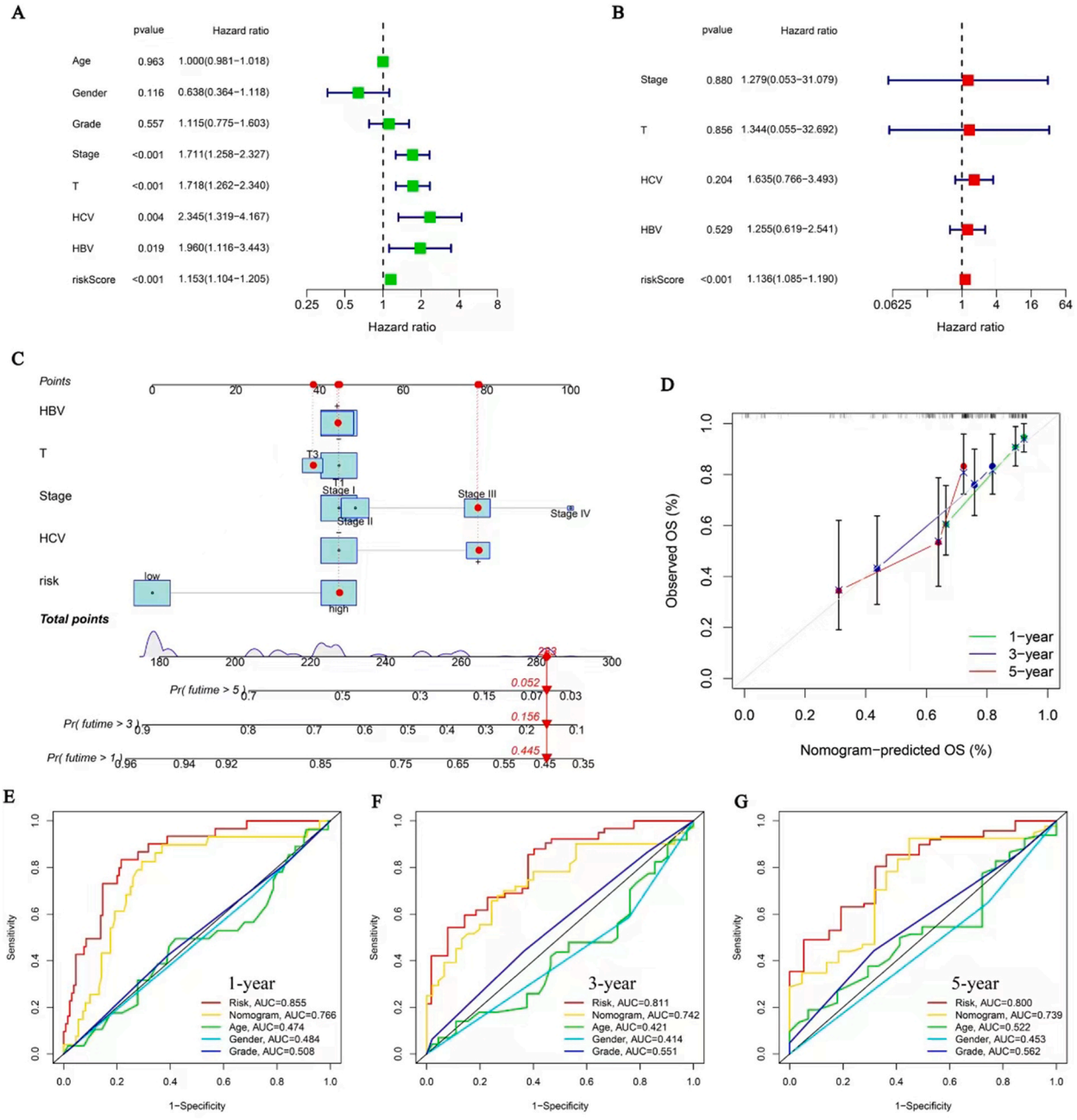

Fig. 5. Construction and assessment of nomogram. (A) Univariate Cox regression analysis. (B) Multivariate Cox regression analysis. (C) Prediction of nomogram in the TCGA-train dataset. (D) Calibration plots for the nomogram. (E, F, G) Multifactor AUC values for 1-year, 3-year, and 5-year survival.

comprehensive analysis unveiled that the cohort of HCC patients harboring diminished risk demonstrated a more auspicious prognostic trajectory compared to their counterparts with elevated risk, a trend that remained consistent across diverse datasets, encompassing TCGA-test, TCGA-all, and ICGC-LIRI-JP (Fig. 3A–C). The AUC values of 1-, 3-, and 5-year in TCGA-test were 0.734, 0.753, and 0.719, respectively (Fig. 3D). The AUC values of 1-, 3-, and 5-year in TCGA-all were 0.810, 0.740, and 0.705, respectively (Fig. 3E). Moreover, in ICGC-LIRI-JP, the AUC values for 1 year, 3 years, and 5 years were 0.672, 0.678, and 0.837, respectively, as depicted in Fig. 3F. We also validated the prognostic predictive capability of the NETs signature across various clinical subgroups within the TCGA dataset. Our results demonstrated that the NETs signature can accurately predict the prognosis of patients in various clinical subgroups, including age >65 ($P = 0.011$), age≤65 ($P < 0.001$), male ($P < 0.001$), G1-2 ($P < 0.001$), G3-4 ($P = 0.027$), N0 ($P < 0.001$), stage I-II ($P = 0.005$), T1-2 ($P < 0.001$), and T3-4 ($P = 0.038$) (Fig. 4). We then compared previously published HCC risk models for accuracy and predictive ability. NETs signature outperformed previously established signatures by calculating and comparing their AUC and C-index values, demonstrating the novel signature may be having a promising predictive application (Supplementary Fig. S1).

3.3. Constructing a novel nomogram for HCC

Both univariate and multivariate analyses consistently demonstrated that our NETs-related signature retains its status as an independent prognostic factor ($P < 0.001$), as supported by the findings in Fig. 5A and B. To optimize the prognostic potential of the NETs signature, we developed an innovative nomogram by integrating the NETs signature and clinical features using the training dataset (Fig. 5C). The calibration curves of the novel nomogram (Fig. 5D) displayed a robust predictive value for prognosis. Furthermore, we compared the prognostic forecasting value of the nomogram with that of clinical characteristics such as gender, grade, and age using ROC analysis. The AUC values at 1-, 3-, and 5-year intervals for the novel nomogram were 0.766, 0.742, and 0.739, respectively (Fig. 5E–G).

To corroborate the aforementioned analytical findings, we proceeded to validate the expression profiles of the differentially expressed genes. Firstly, qRT-PCR experiments were conducted, revealing significantly higher expression of HAVCR1, STC2, CABYR, CYP26B1, and SLC1A5 genes in clinical HCC patient samples compared to the normal group. Conversely, the expression of the CCR7 gene was significantly lower (Fig. 6). Furthermore, the immunohistochemistry staining outcomes provided corroboration for the expressional disparities of the six genes between clinical patients with HCC and the control group (Fig. 7A). Based on the risk coefficients of these differentially expressed genes in HCC (Fig. 2A and B), we selected HAVCR1, which had the highest risk coefficient, for regulation. Specifically, siRNA transfection techniques were employed to interfere with the expression of the HAVCR1 gene in Huh7 cells. The CCK8 experiment results demonstrated that after knocking out the HAVCR1 gene, the proliferation ability of Huh7 cells decreased relative to the negative control group (Fig. 7B). This finding further validates the significant role of the HAVCR1 gene in

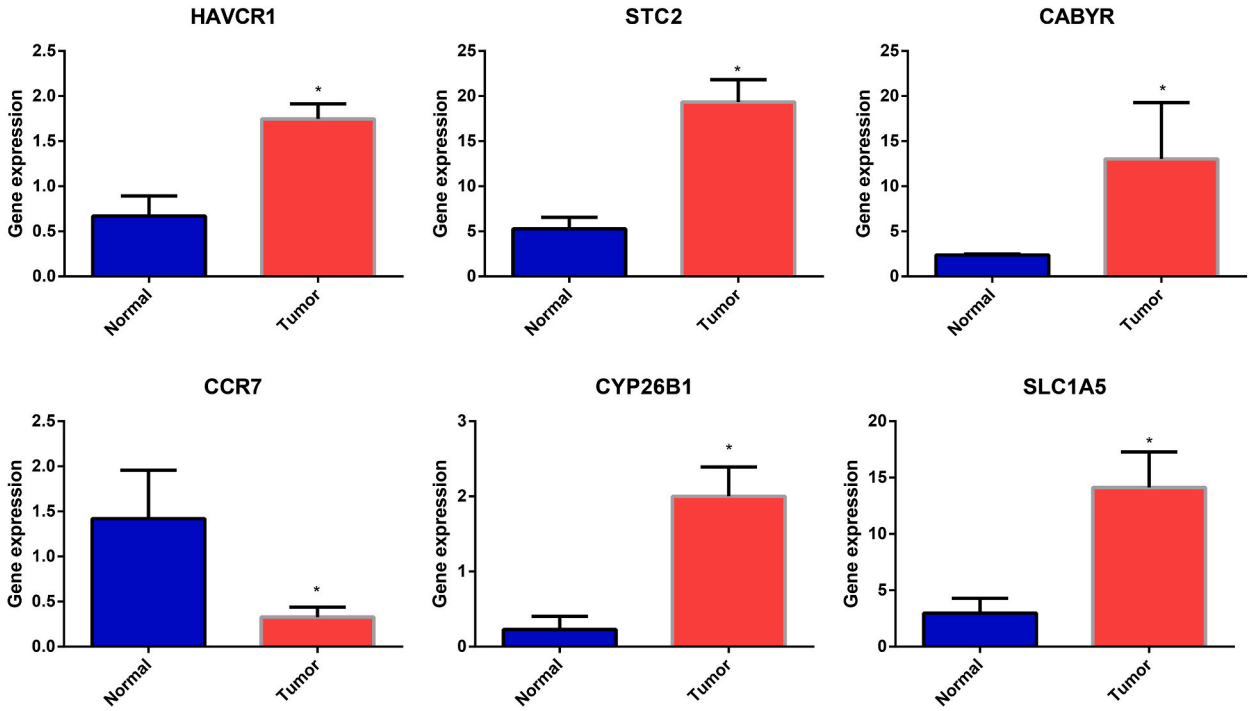

Fig. 6. mRNA expression levels of NETs between the normal group and tumor group. The qRT-PCR experimental results of the genes HAVCR1, STC2, CABYR, CYP26B1, SLC1A5, and CCR7 in clinical samples from patients with HCC.

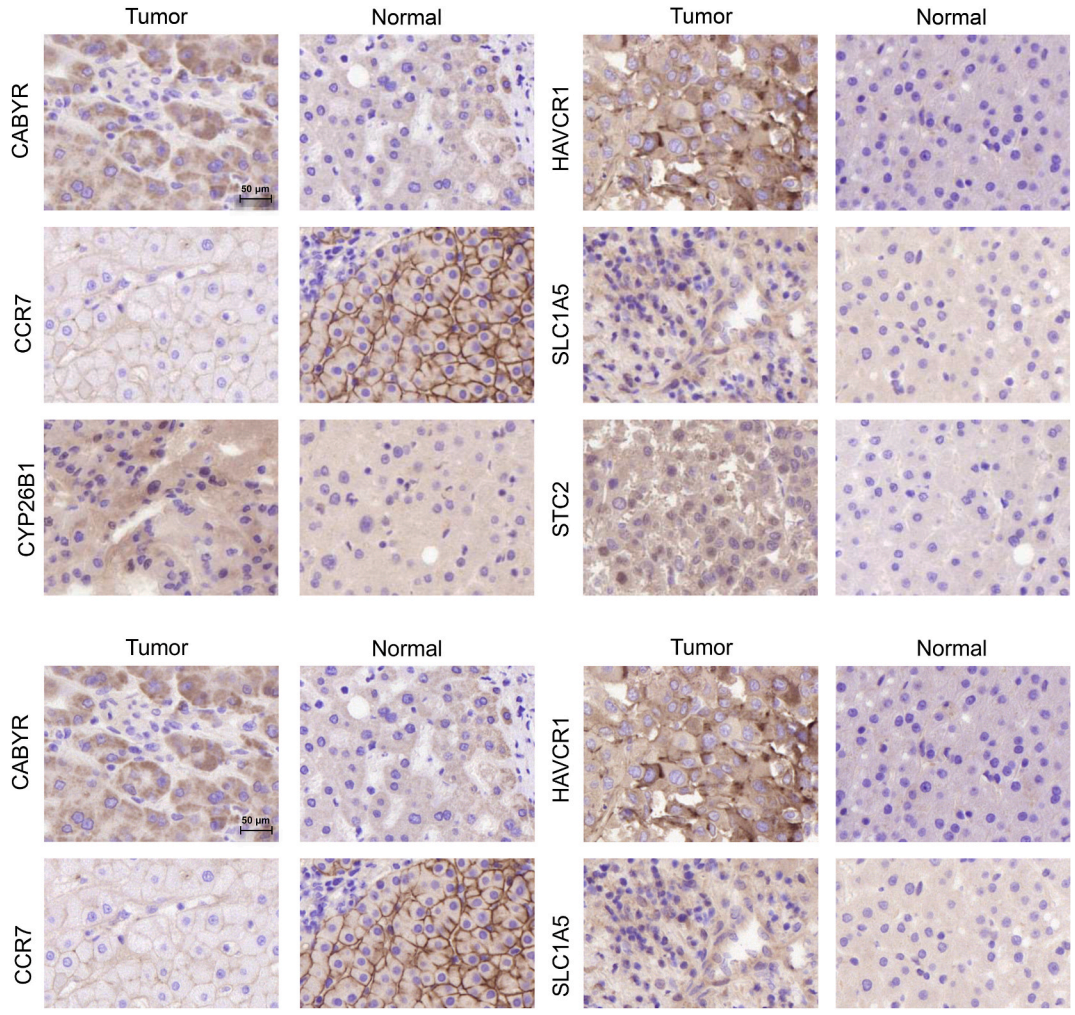

Fig. 7. Comprehensive analysis of NETs protein expression and HAVCR1 regulation. (A) Immunohistochemical staining of CYP26B1, CCR7, CABYR, SLC1A5, HAVCR1, and STC2 in normal group and tumor group. (B) Impact of si-HAVCR1 transfection on cell proliferation in Huh7 cells assessed by cck-8 assay. (C) The levels of NETs specific markers (MPO-DNA complex and NE) in the supernatant of Huh7 cells treated with si-HAVCR1 by ELISA.

HCC cell proliferation. Considering that the level of NET is primarily assessed by measuring the concentrations of MPO and NE [25,26], supernatants from Huh7 cells after si-HAVCR1 transfection were collected, and the levels of MPO and NE were detected using ELISA. A marked reduction in MPO and NE levels was observed in the si-HAVCR1 group relative to the negative control group, as shown in Fig. 7C. This further confirms the regulatory function of the HAVCR1 gene in modulating the level of NET in HCC cells.

These findings suggest that the new nomogram prognostic model based on these six NETs (CYP26B1, CCR7, CABYR, SLC1A5, HAVCR1, and STC2) exhibits excellent predictive performance.

3.4. Evaluation of the tumor microenvironment in two subgroups

HCC is strongly influenced by the tumor microenvironment [27]. According to ESTIMATE analysis, the high-risk group exhibited lower ImuneScores, StromalScores, and ESTIMATEScores (Fig. 8A). ssGSEA analysis found that the high-risk HCC group had lower infiltration levels of NK cells, pDCs, $CD8^+$ T cells, Dendritic Cells (DCs), iDCs, Mast cells, Tfh, Th1, Th2, B cells, Neutrophils, T helper cells, and Tumor-infiltrating lymphocytes (TILs) compared to the low-risk HCC group (Fig. 8B). Low-risk patients demonstrated improved immunologic functions, as evidenced by Fig. 8C. Moreover, the study employed a comprehensive array of methodologies, encompassing MCPCOUNTER, QUANTISEQ, EPIC, XCELL, TIMER, CIBERSORT, and CIBERSORT-ABS, to meticulously examine the variations in immune cell populations between the high-risk and low-risk groups. Fig. 8D illustrates elevated levels of most immune cells in the low-risk group, which may be associated with a better prognosis. In addition, the distribution of high- and low-risk HCC is shown in Fig. 8E.

In the high-risk group, most immune-related genes were low-expressed (Fig. 9A–D). The study investigated the IPS in two

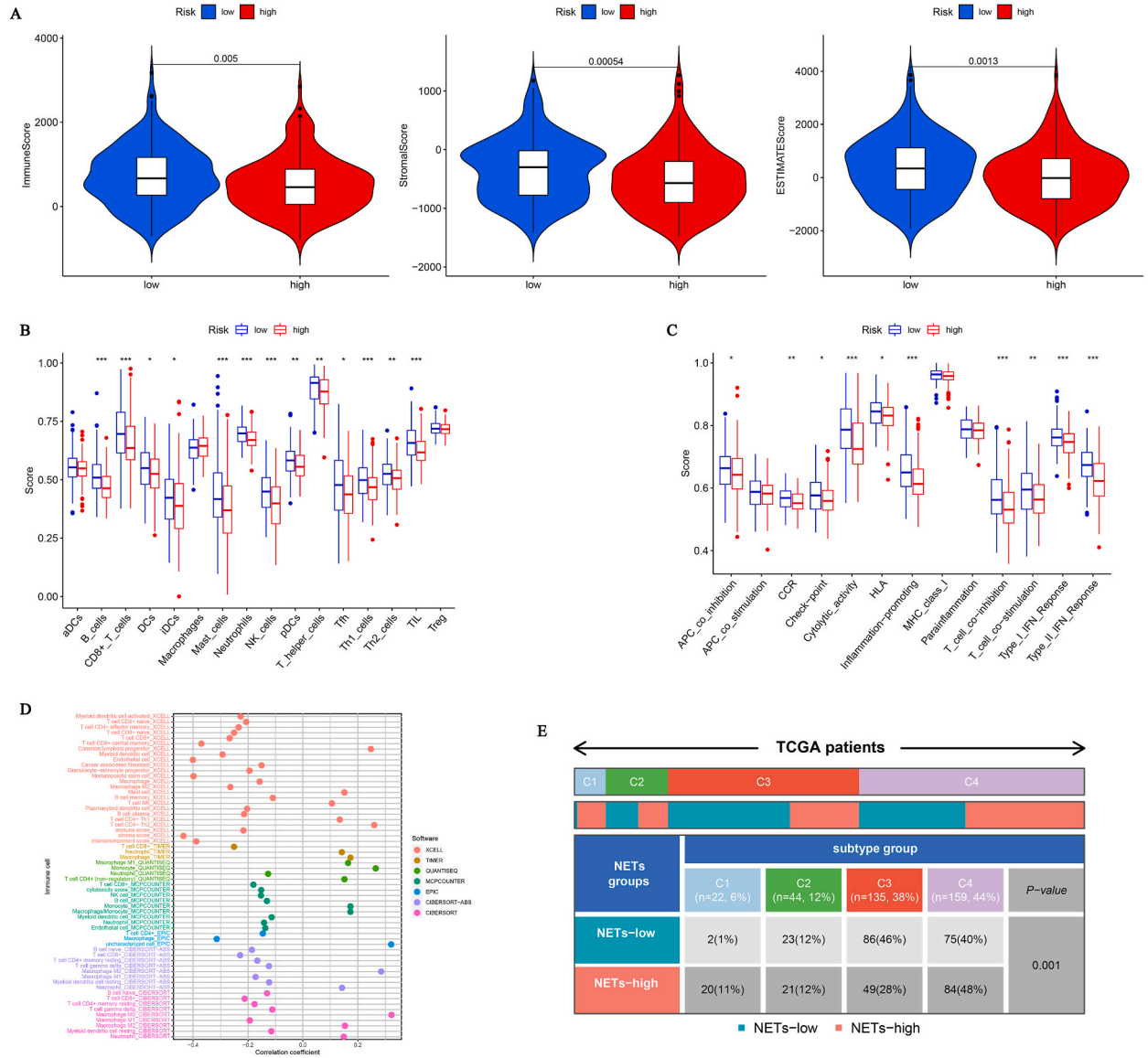

Fig. 8. Analysis of immune conditions of high and low-risk groups. (A) Contrasts in immune microenvironment scores between the two groups. (B) Analysis of variations in immune cell infiltration between the two groups using ssGSEA. (C) Analysis of disparities in immune functions between the two groups using ssGSEA. (D) Comparative analysis of immune cell infiltration between the two groups using multiple algorithms. (E) Distribution of patients with high- and low-risk across different immune subtypes.

subgroups. The findings revealed that the low-risk LIHC subgroup displayed a higher IPS in the CTLA4–PD1+, CTLA4+ PD1–, and CTLA4+ PD1+ groups. This higher IPS indicated a more favorable immunotherapy response, as depicted in Fig. 9E–G. Within the immunotherapy cohort analysis, it was observed that individuals within the low-risk group demonstrated an enhanced responsiveness to immunotherapy interventions (Fig. S2). These results confirmed that low-risk patients respond better to immunotherapy than high-risk patients.

3.5. *Functional evaluation of the NETs signature*

To uncover the molecular underpinnings distinguishing low-risk and high-risk HCC cohorts, we employed the 'limma' R package to identify DEGs. Subsequently, these DEGs were subjected to GO enrichment analysis and KEGG pathway analysis to decipher their functional roles and biological pathways. The results of the GO analysis demonstrated significant enrichment of DEGs in response to xenobiotic stimulus, immunoglobulin complex, and immunoglobulin receptor binding, as depicted in Fig. 10A and B. Similarly, the KEGG analysis revealed a predominant enrichment of DEGs in central carbon metabolism in cancer, the cell cycle, and the HIF-1

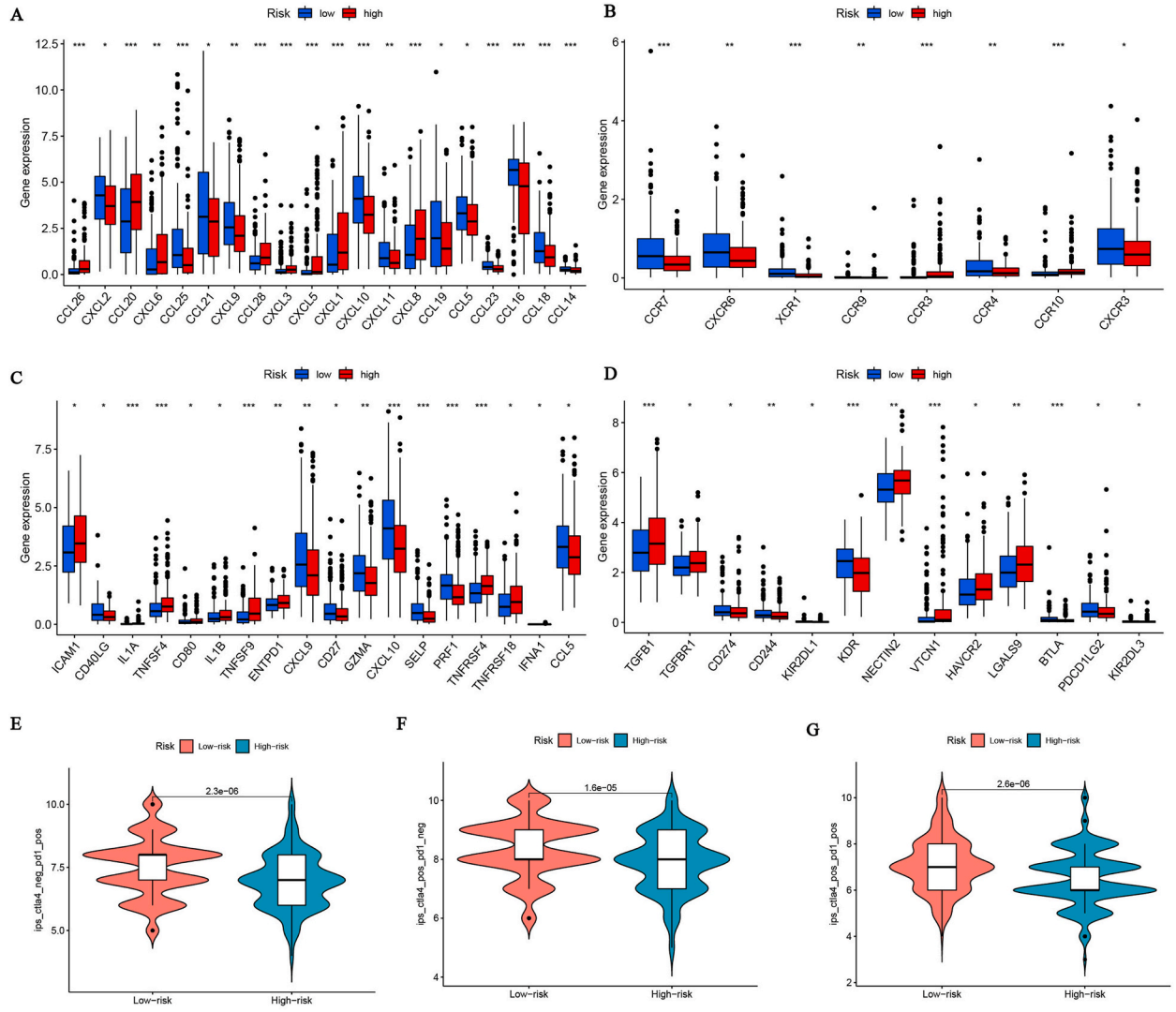

Fig. 9. Assessment of Immunotherapy response of high and low-risk groups. (A–D) Expression levels of immune-related genes in different groups. (E–G) IPS results for low-risk and high-risk LIHC (Liver Hepatocellular Carcinoma) in the following groups: CTLA4 - PD1+ group, CTLA4+ PD1 - group, and CTLA4+ PD1+ group.

signaling pathway, as shown in Fig. 10C and D. Moreover, the GSVA revealed substantial alterations in multiple pathways between high-risk HCC patients and low-risk HCC patients, as illustrated in Fig. 10E.

3.6. Drug sensitivity and risk score correlation analysis

In order to gain deeper insights into the variations in drug sensitivity between HCC patients categorized as high-risk and low-risk, we conducted a comprehensive analysis. Specifically, we explored the relationship between the risk score and the IC50 values of several widely used chemotherapies and targeted therapy drugs. Remarkably, we observed a substantial discrepancy in the IC50 values of 9 drugs (A-443654, AKT inhibitor VIII, PD-173074, BMS-509744, CCT007093, CGP-60474, GSK690693, JNK-9L, and KIN001-102) between the high-risk and low-risk groups (Fig. 11). Strikingly, the IC50 values exhibited a marked reduction in the high-risk group relative to their low-risk counterparts, indicating a heightened sensitivity to the treatment.

4. Discussion

HCC reigns as the predominant form of primary hepatic malignancy. HCC is currently treated primarily with surgery, followed by radiotherapy, chemotherapy, and targeted drugs [28]. However, factors such as recurrence and metastasis make the prognosis of HCC patients poor [29]. NETs can promote the metastasis of liver cancer by stimulating tumor inflammation [30]. The role of NET-related

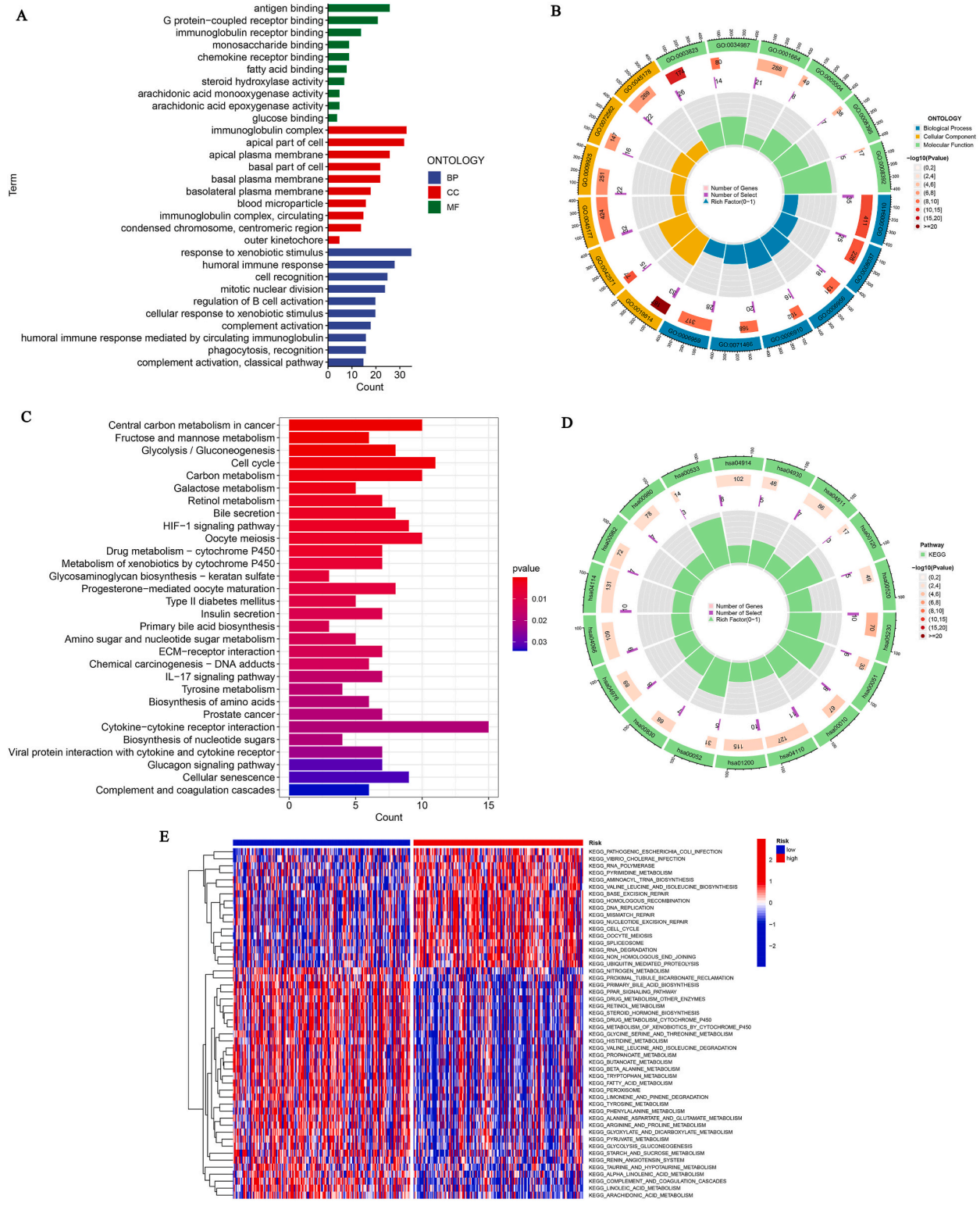

Fig. 10. Function analysis. (A–B) GO analysis comparing the differential gene expression between the high-risk and low-risk groups. (C–D) KEGG analysis comparing the differential gene expression between the high-risk and low-risk groups. (E) GSVA depicting the enrichment analysis in the high-risk and low-risk groups.

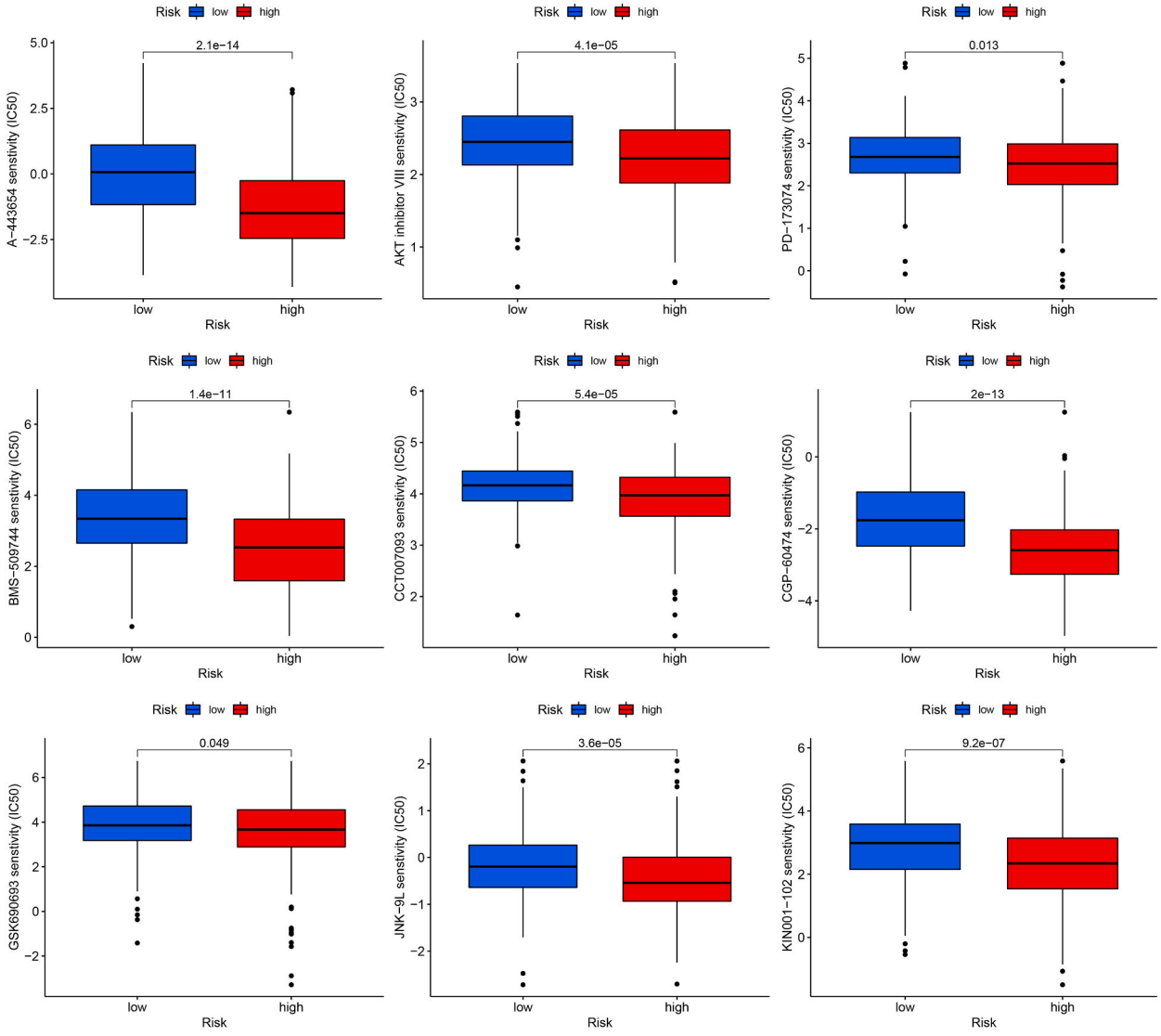

Fig. 11. Drug sensitivity analysis in high and low-risk groups.

genes in the prognosis and immune status of HCC is still unclear. Therefore, identifying a prognostic model of NETs-related genes and judging the prognosis of HCC patients through multiple datasets will help guide clinical decision-making.

In this study, we obtained the HCC-related datasets from TCGA and ICGC databases. Specifically, we downloaded the TCGA-LIHC dataset and subsequently divided it randomly into a training group and a test group. Based on the TCGA-train dataset, we conducted univariate cox regression and lasso analysis to construct a six-gene NETs signature. We evaluated the prognosis of the NETs signature in the TCGA-test, TCGA-all, and ICGC-LIRI-JP datasets. Patients with high-risk disease had significantly shorter overall survival (OS) and poorer survival outcomes compared to those with low-risk HCC. ROC curves for 1-year, 3-year, and 5-year data indicate good specificity and sensitivity for the model. Moreover, an independent prognostic assessment revealed that the model's risk score emerged as an autonomous prognostic determinant, transcending the influence of other clinical parameters. To enhance the utility of the NETs signature, we devised an innovative nomogram that harmoniously integrated clinical characteristics and the risk score of HCC patients. The calibration curve proved a good linear fit of the novel nomogram for predicting prognosis for HCC patients. It is worth noting that qRT-PCR and immunohistochemistry assays reveal a significant difference in the expression of these NETs between patients with liver cancer. Additionally, in vitro experiments targeting the gene with the highest risk coefficient, HAVCR1, confirmed through CCK8 assays and MPO and NE detection, further support the significant role of these NETs in regulating HCC cell proliferation and NET levels. The study identified that the NETs signature could serve as a dependable prognostic indicator for HCC patients, aiding in the development of personalized treatment strategies and offering potential avenues for future basic research on HCC.

The six genes that constitute the prognosis model are CYP26B1, CCR7, CABYR, SLC1A5, HAVCR1, and STC2. These genes are strongly associated with some types of cancer. For example, CYP26B1 plays a new role in the betel quid-dependent pathogenesis of oral

squamous cell carcinoma [31]. Tian et al. elucidated that the expression of CCR7 is elevated in cervical squamous cell carcinoma, harboring prognostic significance for patient survival [32]. CCR7 played an important role in promoting angiogenesis in esophageal squamous cell carcinoma by activating the NF-κB pathway, so CCR7 might be a potential target for anti-angiogenesis therapy in esophageal squamous cell carcinoma [33]. Qian et al. showed that inhibition of CABYR expression increased the chemical sensitivity of lung cancer cells by inhibiting AKT activity [34]. Through the mTOR signaling pathway, ASCT2/SLC1A5 controlled glutamine uptake and tumor progression in triple-negative breast cancers [35]. In addition, Liu et al. found that HAVCR1 was significantly up-regulated in mRNA and protein levels in gastric cancer tissues, and was related to the prognosis of gastric cancer patients [36]. By inducing epithelial-mesenchymal transformation, STC2 was a potential biomarker of pancreatic cancer development [37]. However, the role of these genes in HCC is still insufficient.

The tumor microenvironment (TME) comprises a heterogeneous milieu of immune cells, stromal elements, extracellular matrix components, and tumor-associated vasculature, collectively orchestrating tumorigenesis and cancer progression [38,39]. The levels of immune cells infiltrating the TME typically change as tumors progress [40]. Individuals with low-risk scores demonstrate elevated ImmuneScores, StromalScores, and ESTIMATEScores. Conversely, the high-risk cohort exhibits a notable reduction in immune cell presence compared to the low-risk counterpart. Low-risk patients experience improvements in immunologic functions, while high-risk patients exhibit underexpression of immune-related genes. The proportions of different immune cells are vital for anti-tumor immunity, and the decline in immune cells and function may result in a poor prognosis for high-risk patients. In contrast, the presence of more immune cells in the TME of the low-risk subgroup could be due to their immune system having a stronger response to the tumor. This may be related to the patient's gene expression and the tumor microenvironment. Low-risk patients typically exhibit higher ImuneScores, StromalScores, and ESTIMATEScores, indicating that they have more immune cells and other immune-regulatory components in their TME. Additionally, low-risk patients have higher IPS, indicating that their immune system is more active. Further research is needed to investigate these mechanisms and understand the reasons behind the increased immune cell infiltration in the low-risk subgroup. Our study found that low-risk LIHC patients respond better to immunotherapy than high-risk patients. The IPS, calculated using machine learning, considers effector cells, immunosuppressor cells, MHC molecules, and immunomodulators. This unbiased method has shown the ability to predict a patient's response to immunotherapy [22,23,41]. Our findings posit that low-risk LIHC patients may derive greater therapeutic benefit from immunotherapeutic interventions compared to their high-risk counterparts. These observations have the potential to refine the deployment of immunotherapy and chemotherapy regimens for HCC, while also elucidating the multifaceted role of NETs in the pathogenesis of this disease.

However, there are still some limitations. The majority of analyses rely on data culled from public datasets, with all samples being retrospectively acquired, resulting in inherent case selection bias. Further real-world experiments could verify our analysis.

In conclusion, this study has unveiled a six-gene signature that exhibits robust prognostic utility in predicting the clinical outcomes of HCC patients, including their responsiveness to immunotherapeutic interventions. These insights can illuminate the path towards devising more efficacious treatment strategies and deepen our comprehension of the role of NETs in the pathogenesis of HCC.

Ethics statement

This research endeavor received the imprimatur of the Clinical Ethics Review Committee of Ningbo First Hospital (License number: 068A01; Passed on November 29, 2022). All participants furnished written informed consent.

Funding

The research described in this paper was financially supported by the Ningbo University Institute of Geriatrics (grant number: LNBYJS-2021).

Date availability statement

Data supporting the research findings have been deposited in the approaches and procedures.

CRediT authorship contribution statement

Ziwei Yuan: Writing – original draft. **Xuejia Yang:** Methodology. **Zujian Hu:** Software. **Yuanyuan Gao:** Methodology, Writing – review & editing. **Penghua Yan:** Validation. **Fan Zheng:** Writing – review & editing. **Yangyang Guo:** Project administration, Conceptualization. **Xiaowu Wang:** Formal analysis. **Jingzong Zhou:** Project administration.

Declaration of competing interest

The authors declare that they have no known competing financial interests or personal relationships that could have appeared to influence the work reported in this paper.

Acknowledgement

We extend our heartfelt gratitude to all the individuals whose invaluable contributions made this study possible.

Appendix A. Supplementary data

Supplementary data to this article can be found online at https://doi.org/10.1016/j.heliyon.2024.e30827.

References

[1] F. Bray, J. Ferlay, I. Soerjomataram, R.L. Siegel, L.A. Torre, A. Jemal, Global cancer statistics 2018: GLOBOCAN estimates of incidence and mortality worldwide for 36 cancers in 185 countries, CA A Cancer J. Clin. 68 (6) (2018) 394–424.
[2] A. Villanueva, Hepatocellular carcinoma, N. Engl. J. Med. 380 (15) (2019) 1450–1462.
[3] L. Wang, Q. Li, J. Zhang, J. Lu, A novel prognostic scoring model based on albumin and gamma-glutamyltransferase for hepatocellular carcinoma prognosis, Cancer Manag. Res. 11 (2019) 10685–10694.
[4] D. Dimitroulis, C. Damaskos, S. Valsami, S. Davakis, N. Garmpis, E. Spartalis, A. Athanasiou, D. Moris, S. Sakellariou, S. Kykalos, G. Tsourouflis, A. Garmpi, I. Delladetsima, K. Kontzoglou, G. Kouraklis, From diagnosis to treatment of hepatocellular carcinoma: an epidemic problem for both developed and developing world, World J. Gastroenterol. 23 (29) (2017) 5282–5294.
[5] V. Papayannopoulos, Neutrophil extracellular traps in immunity and disease, Nat. Rev. Immunol. 18 (2) (2018) 134–147.
[6] N.V. Vorobjeva, B.V. Chernyak, NETosis: molecular mechanisms, role in physiology and pathology, Biochemistry (Mosc). 85 (10) (2020) 1178–1190.
[7] B.G. Yipp, P. Kubes, NETosis: how vital is it? Blood 122 (16) (2013) 2784–2794.
[8] U. Demkow, Neutrophil extracellular traps (NETs) in cancer invasion, evasion and metastasis, Cancers 13 (17) (2021) 4495.
[9] K.H. Lee, A. Kronbichler, D.D. Park, Y. Park, H. Moon, H. Kim, J.H. Choi, Y. Choi, S. Shim, I.S. Lyu, B.H. Yun, Y. Han, D. Lee, S.Y. Lee, B.H. Yoo, K.H. Lee, T. L. Kim, H. Kim, J.S. Shim, W. Nam, H. So, S. Choi, S. Lee, J.I. Shin, Neutrophil extracellular traps (NETs) in autoimmune diseases: a comprehensive review, Autoimmun. Rev. 16 (11) (2017) 1160–1173.
[10] S.K. Jorch, P. Kubes, An emerging role for neutrophil extracellular traps in noninfectious disease, Nat. Med. 23 (3) (2017) 279–287.
[11] M.L. De Meo, J.D. Spicer, The role of neutrophil extracellular traps in cancer progression and metastasis, Semin. Immunol. 57 (2021) 101595.
[12] L. Cristinziano, L. Modestino, A. Antonelli, G. Marone, H.U. Simon, G. Varricchi, M.R. Galdiero, Neutrophil extracellular traps in cancer, Semin. Cancer Biol. 79 (2022) 91–104.
[13] L.Y. Yang, Q. Luo, L. Lu, W.W. Zhu, H.T. Sun, R. Wei, Z.F. Lin, X.Y. Wang, C.Q. Wang, M. Lu, H.L. Jia, J.H. Chen, J.B. Zhang, L.X. Qin, Increased neutrophil extracellular traps promote metastasis potential of hepatocellular carcinoma via provoking tumorous inflammatory response, J. Hematol. Oncol. 13 (1) (2020) 3.
[14] Q. Li, W. Chen, Q. Li, J. Mao, X. Chen, A novel neutrophil extracellular trap signature to predict prognosis and immunotherapy response in head and neck squamous cell carcinoma, Front. Immunol. 13 (2022) 1019967.
[15] S. Stelloo, E. Nevedomskaya, Y. Kim, K. Schuurman, E. Valle-Encinas, J. Lobo, O. Krijgsman, D.S. Peeper, S.L. Chang, F.Y. Feng, L.F.A. Wessels, R. Henrique, C. Jeronimo, A.M. Bergman, W. Zwart, Integrative epigenetic taxonomy of primary prostate cancer, Nat. Commun. 9 (1) (2018) 4900.
[16] J. Wang, T. Chen, X. Yu, O.U. N, L. Tan, B. Jia, J. Tong, J. Li, Identification and validation of smoking-related genes in lung adenocarcinoma using an in vitro carcinogenesis model and bioinformatics analysis, J. Transl. Med. 18 (1) (2020) 313.
[17] R. Zhu, H. Tao, W. Lin, L. Tang, Y. Hu, Identification of an immune-related gene signature based on immunogenomic landscape analysis to predict the prognosis of adult acute myeloid leukemia patients, Front. Oncol. 10 (2020) 574939.
[18] K. Sha, Y. Lu, P. Zhang, R. Pei, X. Shi, Z. Fan, L. Chen, Identifying a novel 5-gene signature predicting clinical outcomes in acute myeloid leukemia, Clin. Transl. Oncol. 23 (3) (2021) 648–656.
[19] J. Xiong, S. Guo, Z. Bing, Y. Su, L. Guo, A comprehensive RNA expression signature for cervical squamous cell carcinoma prognosis, Front. Genet. 9 (2018) 696.
[20] K. He, S. Liu, Y. Xia, J. Xu, F. Liu, J. Xiao, Y. Li, Q. Ding, L. Lu, G. Xiang, M. Zhan, CXCL12 and IL7R as novel therapeutic targets for liver hepatocellular carcinoma are correlated with somatic mutations and the tumor immunological microenvironment, Front. Oncol. 10 (2020) 574853.
[21] X. Zhang, L. Li, P. Liu, Y. Tian, P. Gong, Development of a transcription factor-based prognostic model for predicting the immune status and outcome in pancreatic adenocarcinoma, J Immunol Res 2022 (2022) 4946020.
[22] C. Li, Y. Tang, Q. Li, H. Liu, X. Ma, L. He, H. Shi, The prognostic and immune significance of C15orf48 in pan-cancer and its relationship with proliferation and apoptosis of thyroid carcinoma, Front. Immunol. 14 (2023) 1131870.
[23] C.P. Gui, J.H. Wei, Y.H. Chen, L.M. Fu, Y.M. Tang, J.Z. Cao, W. Chen, J.H. Luo, A new thinking: extended application of genomic selection to screen multiomics data for development of novel hypoxia-immune biomarkers and target therapy of clear cell renal cell carcinoma, Briefings Bioinf. 22 (6) (2021) bbab173.
[24] S. Wang, G. Guan, C. Zou, Q. Guo, W. Cheng, S. Shen, F. Dong, A. Wu, G. Li, C. Zhu, Genome profiling of mismatch repair genes in eight types of tumors, Cell Cycle 20 (11) (2021) 1091–1106.
[25] V. Papayannopoulos, K.D. Metzler, A. Hakkim, A. Zychlinsky, Neutrophil elastase and myeloperoxidase regulate the formation of neutrophil extracellular traps, J. Cell Biol. 191 (3) (2010) 677–691.
[26] V. Brinkmann, U. Reichard, C. Goosmann, B. Fauler, Y. Uhlemann, D.S. Weiss, Y. Weinrauch, A. Zychlinsky, Neutrophil extracellular traps kill bacteria, Science 303 (5663) (2004) 1532–1535.
[27] Y. Hu, H. Sun, H. Zhang, X. Wang, An immunogram for an individualized assessment of the antitumor immune response in patients with hepatocellular carcinoma, Front. Oncol. 10 (2020) 1189.
[28] P. Ganesan, L.M. Kulik, Hepatocellular carcinoma: new developments, Clin. Liver Dis. 27 (1) (2023) 85–102.
[29] J.K.H. Liu, A.F. Irvine, R.L. Jones, A. Samson, Immunotherapies for hepatocellular carcinoma, Cancer Med. 11 (3) (2022) 571–591.
[30] D.J. van der Windt, V. Sud, H. Zhang, P.R. Varley, J. Goswami, H.O. Yazdani, S. Tohme, P. Loughran, R.M. O'Doherty, M.I. Minervini, H. Huang, R.L. Simmons, A. Tsung, Neutrophil extracellular traps promote inflammation and development of hepatocellular carcinoma in nonalcoholic steatohepatitis, Hepatology 68 (4) (2018) 1347–1360.
[31] P.H. Chen, K.W. Lee, C.H. Chen, T.Y. Shieh, P.S. Ho, S.J. Wang, C.H. Lee, S.F. Yang, M.K. Chen, S.L. Chiang, Y.C. Ko, CYP26B1 is a novel candidate gene for betel quid-related oral squamous cell carcinoma, Oral Oncol. 47 (7) (2011) 594–600.
[32] W.J. Tian, P.H. Feng, J. Wang, T. Yan, Q.F. Qin, D.L. Li, W.T. Liang, CCR7 has potential to Be a prognosis marker for cervical squamous cell carcinoma and an index for tumor microenvironment change, Front. Mol. Biosci. 8 (2021) 583028.
[33] Q.Y. Cai, G.Y. Liang, Y.F. Zheng, Q.Y. Tan, R.W. Wang, K. Li, CCR7 enhances the angiogenic capacity of esophageal squamous carcinoma cells in vitro via activation of the NF-kappaB/VEGF signaling pathway, Am J Transl Res 9 (7) (2017) 3282–3292.
[34] Z. Qian, M. Li, R. Wang, Q. Xiao, J. Wang, M. Li, D. He, X. Xiao, Knockdown of CABYR-a/b increases chemosensitivity of human non-small cell lung cancer cells through inactivation of Akt, Mol. Cancer Res. 12 (3) (2014) 335–347.
[35] M. van Geldermalsen, Q. Wang, R. Nagarajah, A.D. Marshall, A. Thoeng, D. Gao, W. Ritchie, Y. Feng, C.G. Bailey, N. Deng, K. Harvey, J.M. Beith, C.I. Selinger, S. A. O'Toole, J.E. Rasko, J. Holst, ASCT2/SLC1A5 controls glutamine uptake and tumour growth in triple-negative basal-like breast cancer, Oncogene 35 (24) (2016) 3201–3208.
[36] L. Liu, Z. Song, Y. Zhao, C. Li, H. Wei, J. Ma, Y. Du, HAVCR1 expression might be a novel prognostic factor for gastric cancer, PLoS One 13 (11) (2018) e0206423.
[37] C. Lin, L. Sun, S. Huang, X. Weng, Z. Wu, STC2 is a potential prognostic biomarker for pancreatic cancer and promotes migration and invasion by inducing epithelial-mesenchymal transition, BioMed Res. Int. 2019 (2019) 8042489.

[38] M. Yang, J. Li, P. Gu, X. Fan, The application of nanoparticles in cancer immunotherapy: targeting tumor microenvironment, Bioact. Mater. 6 (7) (2021) 1973–1987.
[39] D.C. Hinshaw, L.A. Shevde, The tumor microenvironment innately modulates cancer progression, Cancer Res. 79 (18) (2019) 4557–4566.
[40] J.E. Bader, K. Voss, J.C. Rathmell, Targeting metabolism to improve the tumor microenvironment for cancer immunotherapy, Mol. Cell 78 (6) (2020) 1019–1033.
[41] J. Wu, L. Li, H. Zhang, Y. Zhao, H. Zhang, S. Wu, B. Xu, A risk model developed based on tumor microenvironment predicts overall survival and associates with tumor immunity of patients with lung adenocarcinoma, Oncogene 40 (26) (2021) 4413–4424.